Self-Association and DNA Binding of λ cI Repressor N-Terminal Domains Reveal Linkage between Sequence-Specific Binding and the C-Terminal Cooperativity Domain†

David L. Bain and Gary K. Ackers*

Department of Biochemistry and Molecular Biophysics, Washington University School of Medicine, St. Louis, Missouri 63110

Received April 5, 1994; Revised Manuscript Received September 13, 1994®

ABSTRACT: The effects of temperature, protons, and KCl on self-assembly and site-specific binding of λ cI N-terminal domains with operator sites O_R were studied to assess the roles of these domains in DNA binding and cooperativity of the natural system. Domain self-assembly was studied using sedimentation equilibrium while domain−O_R interactions were analyzed by quantitative DNase footprint titration. The self-assembly reactions were modeled best as a monomer−dimer−tetramer stoichiometry. Compared with intact cI, the monomer−dimer assembly is energetically weak and is largely independent of pH and KCl. The van't Hoff enthalpy of dimerization was found to be large and positive (+10.8 kcal/mol), in sharp contrast to that of intact cI (i.e., −16.1 kcal/mol; Koblan & Ackers, 1991a), indicating that different driving forces dominate the respective assembly processes. The interactions of O_R with N-terminal domains were noncooperative under all conditions studied. Binding at each site is accompanied by a negative enthalpy (large at site 1, small at sites 2 and 3). Identical values for salt release and proton absorption were found for the three sites. Comparisons with the analogous thermodynamic parameters from our previous studies indicate that N-terminal domains exhibit different linkages to pH, KCl, and *T* from those of intact cI−O_R interactions. This implies that the domains do not act independently within the intact repressor. Since the linkage differences are dependent upon which site the proteins are binding, the C-terminal domain must play a role in repressor discrimination between specific sites.

Regulation of transcriptional initiation involves complex interactions of proteins binding at specific DNA sequences as well as cooperative interactions between the protein components. Even the simplest systems involve protein self-association and binding to multiple operator sites. Although much work has been done on elucidating the rules and chemical forces by which proteins recognize and bind DNA, a corresponding knowledge of cooperativity effects is still being developed. An emerging picture indicates that it may be difficult to interpret such interactions in terms of a sum of local effects. One approach to elucidating the mechanism(s) by which cooperatively interacting systems regulate biological function is to determine the energetics of each macromolecular interaction over a range of conditions. Such a thermodynamic "dissection" of the functional energetics may then allow resolution of the physicochemical forces which control self assembly, cooperativity, and site-specific binding.

A research program of this laboratory has been focused on interactions at the right operator O_R of bacteriophage λ [see Koblan and Ackers (1992) and references therein, Beckett et al. (1993), Burz et al. (1994), and Burz and Ackers (1994)]. This system has served as a prototype for cooperatively interacting gene regulatory switches. Two viral repressor proteins, cI and cro, interact with three operator sites of O_R to regulate the transition from the lysogenic state to the lytic phase of the bacteriophage life cycle [see Ptashne (1986) for a review]. This protein−DNA complex serves as a molecular switch between different modes of growth based upon two critical features: (1) differential affinity of cI and cro for the three DNA binding sites of O_R and (2) cooperative interactions between adjacently bound cI molecules. The footprint titration technique, a quantitative method for measuring individual-site binding energetics, allows resolution of intrinsic binding free energies as well as cooperative free energies. Since cI repressor and the DNA binding domain of cI repressor (N-terminal domain) bind DNA as dimers, the dimerization reaction must be quantitated in order to obtain accurate binding free energies. Consequently, sedimentation equilibrium was used to evaluate self-assembly of the N-terminal domains. The dimerization energetics of intact cI repressor have been characterized previously over the same ranges of conditions (Koblan & Ackers, 1991a).

In the present work, interactions of cI repressor N-terminal domains with O_R were studied as a function of pH (5−8), temperature (5−37 °C), and monovalent salt (50−200 mM KCl). The goal was to assess the role of N-terminal domains in DNA binding and cooperativity of the natural system. By driving the system with different chemical potentials, one can determine the contributions of protons and other ions to self-assembly and DNA binding. Temperature studies similarly allow resolution of the enthalpic and entropic contributions. This database, in conjunction with previous studies of cI−O_R interactions (Brenowitz et al., 1986; Senear & Ackers, 1990; Koblan & Ackers, 1991a,b, 1992) may lend insight into the nature of cooperativity and site specificity in gene regulatory systems.

† This work was supported by NIH Grants GM39343 and R37GM24486 (G.K.A.).

* Author to whom correspondence should be addressed.

® Abstract published in *Advance ACS Abstracts,* November 1, 1994.

0006-2960/94/0433-14679$04.50/0

MATERIALS AND METHODS

Chemical Reagents. α-^{32}P-Labeled deoxyribonucleotides (3000 Ci/mmol) were from Amersham; unlabeled deoxyribonucleotides were from P-L Biochemicals. Electrophoresis-grade acrylamide, bis(acrylamide), ammonium persulfate, and TEMED were from Bio-Rad. Urea was sequenal grade from Pierce Chemical Co. All other compounds were reagent or analytical grade. Acrylamide, bis(acrylamide), and urea were deionized with Bio-Rad AG501-X8 resin prior to use.

Biological Materials. Restriction endonucleases were from IBI. The large (Klenow) fragment of *Escherichia coli* DNA polymerase I and bovine serum albumin (BSA) (acetylated nucleic acid enzyme grade) were from Bethesda Research Labs. Calf thymus DNA (CT-DNA) was from P-L Biochemicals. Bovine pancreas deoxyribonuclease I (DNase I, code D) from Worthington was stored as a 2 mg/mL stock solution in 150 mM NaCl and 50% glycerol at −70 °C and diluted appropriately into assay buffer less BSA and CT-DNA, immediately prior to use. The relative catalytic activity of DNase I was determined at each condition in order to obtain constant backbone nicking. The nicking pattern was similar under all conditions, indicating no significant conformational changes of the protein−DNA complexes.

Bacterial strain X90 containing plasmid pWL105 encoding the N-terminal domain (1−102 aa) was kindly donated by Dr. Robert Sauer. Domains were purified according to a procedure previously described (Sauer et al., 1986). Protein was judged to be greater than 95% pure based on SDS−PAGE and analytical HPLC. An extinction coefficient of 0.58/mg/(mL·cm) was calculated. [This value is in close agreement with that of Weiss et al. (1987).] An extinction coefficient was also measured experimentally by analytical ultracentrifugation (Beckman Model E equipped with interference optics) following the method of Babul and Stellwagon (1969). The resolved value was 0.6/mg/(mL·cm), in close agreement with estimated values.

Repressor−DNA binding activity was measured by isothermal titration calorimetry (Wiseman et al., 1989). Purified protein was titrated with an O_R1 21-bp oligomer synthesized by Oligos etc. DNA binding activity was determined to be 68 ± 10%. Total active monomer concentration was calculated from calorimetry results. Active free dimer concentration was calculated on the basis of the monomer−dimer equilibrium constant determined at each condition studied.

Preparation of Operator DNA. Plasmids pKB252, pBJ301, and pBJ303 contain the three O_R DNA fragments used in the footprint titration studies (Backman et al., 1976; Meyer et al., 1980). pKB252 contains the wild-type O_R template (O_R+). pBJ301 and pBJ303 contain reduced-valency mutant templates in which a single base-pair change has been made in one or two DNA binding sites that eliminate or greatly reduce cI repressor ligation. pBJ301 contains a mutation in site 1 (O_R1−), and pBJ303 contains mutations in sites 1 and 3 (O_R1−,3−). All fragments were excised with a *Pst*I and *Bgl*II digestion, resulting in 1102-bp fragments. All DNA fragments were purified and radiolabeled according to standard procedures (Maniatis et al., 1982). Specific radioactivity of freshly labeled fragments was in the range of (7−10) × 10^6 Ci/mol.

Individual-Site Binding Experiments. Quantitative DNase I footprint titration experiments were performed essentially as described (Brenowitz et al., 1986). The assay buffer for each salt study consisted of 10 mM Bistris, 2.5 mM $MgCl_2$, 1.0 mM $CaCl_2$, 100 μg/mL BSA, 2 μg/mL CT-DNA (sonicated), pH 7.00 ± 0.01, and 50−200 mM KCl. Assay buffer for pH studies contained 10 mM Tris (pH 8.00 ± 0.01), Bistris (pH 7.00, pH 6.00) or acetate (pH 5.00), 200 mM KCl, 2.5 mM $MgCl_2$, 1.0 mM $CaCl_2$, 100 μg/mL BSA, and 2 μg/mL CT-DNA (sonicated). Assay buffer for temperature studies contained 10 mM Bistris, 2.5 mM $MgCl_2$, 1.0 mM $CaCl_2$, 100 μg/mL BSA, and 2 μg/mL CT-DNA (sonicated), and the pH was adjusted to 7.00 ± 0.01 at each temperature. Domains and O_R DNA (15 000−25 000 cpm) were equilibrated in 100-μL volumes for at least 1 h at either 20 °C (for salt and pH studies) or at the appropriate temperature for temperature studies. Upon addition of 2.5 μL of DNase I, the reaction was allowed to proceed for exactly 1 min. The reaction was stopped by addition of 20 μL of 50 mM EDTA, pH 8.0, followed by addition of the standard ethanol cold quench. Electrophoresis of digested DNA on 8% acrylamide−urea gels followed by autoradiography was as described previously (Brenowitz et al., 1986).

Films were scanned in two dimensions in order to determine accurately the fractional saturation at each binding site. Film optical density was determined using an Eikonix 1412 CCD digital imaging camera. The optical density was normalized to 256 gray levels. Digitized films were resolved to 150 μm × 150 μm pixel size. Camera response was determined to be linear up to 2.2 optical density units, well beyond linear film response. The scanned film was processed interactively with programs developed in this laboratory. Fractional saturation was determined as described previously (Brenowitz et al., 1986).

The signal in a footprint titration experiment is the extent of protection at each site from DNase I nicking afforded by a given concentration of repressor. Protection at each site is directly proportional to the fractional saturation at that site. However, since even a saturating ligand concentration does not offer complete protection from DNase, the apparent fractional saturation does not span the range from 0 to 1. Therefore, each isotherm must be analyzed as a transition curve, where the end points are treated as adjustable parameters to be resolved by least-squares analysis. This approach requires that the titration of sites be conducted over a large concentration range (typically 6−10 orders of magnitude) in order to determine reliable transition end points and accurate binding energetics.

Numerical Analysis. Data were analyzed with the appropriate binding functions using nonlinear least-squares parameter estimation (Johnson & Frasier, 1985) to determine the best-fit model-dependent parameters which yield a minimum in the variance. A resolved variance ratio is predicted by an F statistic (Box, 1960) to determine the worst case joint confidence intervals for the fitted parameters. Confidence intervals (67%) correspond to approximately one standard deviation.

Due to the high correlation between constants being resolved, one must analyze simultaneously data of appropriate sets of operator templates in order to obtain physically meaningful microscopic Gibbs binding free energies. This approach holds true even for studying noncooperative systems; one cannot determine whether a protein−DNA system is noncooperative or cooperative by studying only interactions with the wild-type operator. Independent data

Table 1: Microscopic Configurations and Associated Free Energy Contributions for the System Containing λ cI N-Terminal Domains and DNA Operator Sites, O_R[a]

species	operator configurations O_R1		O_R2		O_R3	free energy contributions
1	0		0		0	reference
2	R_2		0		0	ΔG_1
3	0		R_2		0	ΔG_2
4	0		0		R_2	ΔG_3
5	R_2	↔	R_2		0	$\Delta G_1 + \Delta G_2 + \Delta G_{12}$
6	R_2		0		R_2	$\Delta G_1 + \Delta G_3$
7	0		R_2	↔	R_2	$\Delta G_2 + \Delta G_3 + \Delta G_{23}$
8	R_2	↔	R_2		R_2	$\Delta G_1 + \Delta G_2 + \Delta G_3 + \Delta G_{12}$

[a] Individual operator sites are denoted by 0 if vacant or by R_2 if occupied by N-terminal domain dimers. Cooperative interactions are denoted (↔). ΔG_i values (i = 1, 2, or 3) are the intrinsic Gibbs free energies for binding to each of the three operator sites. ΔG_{ij} values are the free energies of cooperative interaction between adjacent liganded sites. The free energies are related to the corresponding microscopic equilibrium constants, k_i, by the standard relationship $\Delta G_i = -RT \ln k_i$.

sets are analyzed as a composite in order to resolve the model parameters that simultaneously minimize the variance for the entire data set. In order to resolve the five microscopic interaction constants, this study used the wild-type template (O_R+) and two well-studied "reduced valency" templates, O_R1- and $O_R1-,3-$. A critical assumption for this type of analysis is that intrinsic interactions at any competent binding site are unperturbed by the mutation(s) introduced at the other site(s). The validity of this assumption has been explored for interactions of cI repressor and O_R (Senear & Ackers, 1990; Koblan & Ackers, 1991b, 1992; Burz & Ackers, 1994).

At each pH studied, the five parameters of Table 1 were resolved by simultaneous analysis of duplicate experiments of O_R+ templates and the two reduced valency templates discussed above. The same approach was used for extremes of salt concentration (50 and 200 mM KCl) and temperature (5 and 37 °C). As there was no evidence for cooperative interactions under any condition, duplicate experiments using only O_R+ templates were analyzed for intermediate salt concentrations (100 and 150 mM KCl) and temperature (10 and 30 °C) studies. The cooperative free energies were set equal to zero at these conditions. No weighting factors were employed in any analysis.

At all conditions the approximation that $[P]_{total} \approx [P]_{free}$ is accurate because operator concentrations were low relative to the equilibrium constants. Free dimer concentrations were calculated directly from the truncated repressor conservation equation $R_t = R_1 + 2R_2$ (monomer units) and knowledge of the dimerization constant from the sedimentation equilibrium studies.

Interaction Free Energies. Gibbs energies for both site-specific repressor binding and pairwise interactions were determined by analyzing data according to the equations appropriate for the various individual sites. These equations are formulated from the relative probabilities, f_s, of each microscopic operator configuration:

$$f_s = \exp(-\Delta G_s/RT)[R_2]^j / \sum \exp(-\Delta G_s/RT)[R_2]^j \quad (1)$$

ΔG_s is the sum of free energy contributions for configuration s (Table 1), R the gas constant, T the absolute temperature. $[R_2]$ the free dimer concentration, and j the repressor stoichiometry in operator configuration s. Interactions of the N-terminal domains with the three operator sites yield eight configurations of occupancy (Table 1) (Shea, 1983). Among these configurations the pairwise interactions between occupied sites define an "alternate pairwise cooperativity" model (Johnson et al., 1979). Five microscopic free energy terms can contribute to each species, ΔG_s. These free energies, ΔG_1, ΔG_2, and ΔG_3, reflect binding to each respective site in the absence of binding at any other sites. Cooperativity terms ΔG_{12} and ΔG_{23} represent the excess free energy for binding to two sites simultaneously. By definition ΔG_{ij} is the difference between the total free energy to fill two adjacent sites i and j simultaneously (ΔG_T) and the sum of intrinsic binding energies ($\Delta G_i + \Delta G_j$). The DNase I footprint titration technique resolves the fractional occupancies of each operator site, Y_i, as a function of $[R_2]$, the concentration of unbound dimer. Mathematical expressions for the individual-site isotherms are constructed by summation of the probabilities f_s, for the respective configurations of Table 1 (e.g., for a wild-type operator):

$$Y_{O_R1} = f_2 + f_5 + f_6 + f_8 \quad (2a)$$

$$Y_{O_R2} = f_3 + f_5 + f_7 + f_8 \quad (2b)$$

$$Y_{O_R3} = f_4 + f_6 + f_7 + f_8 \quad (2c)$$

Relationships were obtained in an analogous manner for mutant operators where specific binding sites have been eliminated by single base-pair substitutions. For example, only configurations 1, 3, 4, and 7 (Table 1) can exist for an O_R1- mutant operator.

Previous studies from this laboratory have examined various models to describe footprint titration data (e.g., the "alternate pairwise", "extended pairwise", and "general cooperativity" models). Data in this study were analyzed by the alternate pairwise model (Table 1) and also by the general model (Senear & Ackers, 1990) to test for absence of significant cooperativity and for robustness of values for intrinsic binding constants. It was found that the general model incorporating a ΔG_{123} term resulted in free energies identical to those from the alternate pairwise model analysis (Table 5).

Figure 1 presents a representative set of footprint titrations to O_R+ and reduced valency templates O_R1- and O_R1-, 3−. Data were analyzed simultaneously, using the respective binding expressions in the form of eq 2. Symbols represent individual data points. Each curve represents an isotherm for each operator site calculated using the resolved parameters from the simultaneous analysis. Under most conditions studied, protection at regions outside the operator sites was not observed, indicative of the high specificity or repressor domains. Nonspecific binding could be detected only at low salt conditions (50 mM KCl) and low pH (pH 5). Even at those conditions, however, the site-specific titrations were complete before nonspecific binding became a significant factor. This suggests that the intrinsic free energy of nonspecific binding is similar to that of intact repressor once the weak dimerization free energy is accounted for.

Sedimentation Equilibrium Studies. Sedimentation equilibrium was used to determine the dimerization constant of cI N-terminal domains at all conditions studied in the DNase I footprint titration experiments. Experiments were carried

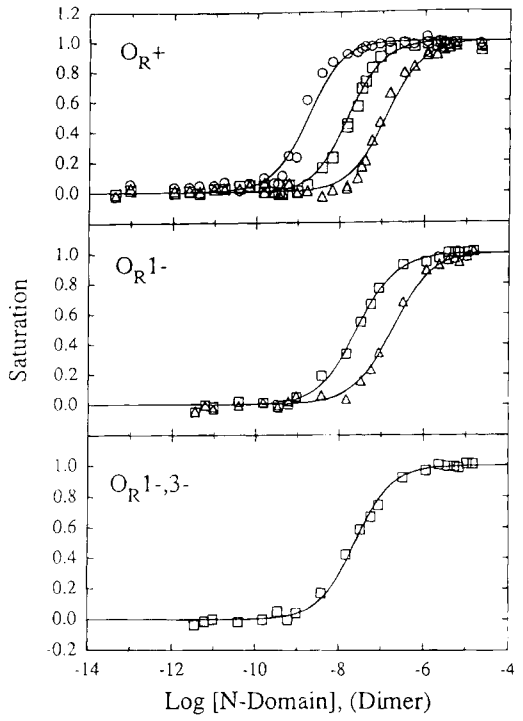

FIGURE 1: Individual-site binding data for interaction of λ cI N-terminal domains with O_R+ and reduced valency O_R mutants. Panels show O_R+, O_R1−, and O_R1−,3− operators, respectively. Symbols: (○) site O_R1; (□) site O_R2; (△) site O_R3. Solid curves represent simultaneous analysis of the data in all panels. Reaction conditions: 37 °C, pH 7, 200 mM KCl.

out with a Beckman XL-A Ultima analytical ultracentrifuge equipped with a Ti-60a titanium four-hole rotor with two-channel, 12-mm path-length centerpieces. Absorbance optics were used throughout. The spectrophotometer had a linear response up to ~1.7 optical density units as judged by monitoring the 280/290 nm ratio as a function of the radius. No data set was analyzed if the absorbance was above 1.7, nor was any data used when the absorbance was less than 0.1. Protein was either dialyzed or diluted into appropriate buffer [identical to the buffer(s) used in footprinting experiments less BSA and CT-DNA]. Three different protein concentrations were used with ratios of 1:3:10. The highest protein concentration was 400 μM (4.5 mg/mL). Sample volume ranged from 150 to 200 μL. Samples were run at 10K, 15K, and 20K rpm. Runs at higher speeds were judged unacceptable due to massive aggregation in the >5 mg/mL range. [As seen also by Weiss et al. (1987) in NMR experiments.] The density (ϱ) of each buffer solution was calculated on the basis of the salt composition and equilibrium temperature. The partial specific volume ($\bar{v}$) of the protein (0.742 mL/g) was calculated by summing the partial specific volumes of the individual amino acids (Cohn & Edsall, 1943). Samples were judged to be at equilibrium by overlaying successive scans. Samples took approximately 20 h to reach equilibrium. Each data point was an average of four scans. Scans were taken every 0.001 cm. Data were selected for analysis using the program REEDIT (generously provided by Dr. David Yphantis). Simultaneous analysis of nine channels (three concentrations at three speeds) was carried out to resolve stoichiometry and equilibrium constants. Data were analyzed using the appropriate functions by nonlinear least-squares parameter estimation (Johnson & Frasier, 1985) to determine the best-fit model-dependent

Table 2: Concentration Dependence of Apparent Molecular Weight Average for N-Terminal Domains at pH 7, 200 mM KCl, and 20 °C

speed (rpm)	λ (nm)	[cI] (μM)[a]	M_r[b]	s[c]
10 000	290	324 (250, 403)	27 570 ± 2400	0.003
10 000	280	85.7 (64, 116)	19 414 ± 1000	0.004
10 000	280	28.3 (22.5, 36.1)	19 148 ± 1500	0.002
15 000	290	253 (165, 428)	27 127 ± 1800	0.004
15 000	280	77.9 (45, 142)	17 818 ± 500	0.004
15 000	280	26.7 (17.0, 43.1)	15 780 ± 1000	0.003
20 000	290	158 (76.5, 393)	23 403 ± 1000	0.004
20 000	280	57.1 (24, 156)	16 755 ± 300	0.005
20 000	280	21.0 (9.8, 52)	15 514 ± 600	0.003

[a] Estimated midchannel protein concentration. Concentration at meniscus and base given in parentheses. [b] Estimated weight average molecular weight ±67% confidence intervals. Molecular weight resolved by assuming no self-assembly reactions. Increase in apparent molecular weight as a function of protein concentration indicative of self-assembly. [c] Square root of variance (optical density units).

parameters that minimize the variance. The program NONLIN was used (Johnson et al., 1981; kindly donated by Dr. David Yphantis). Confidence intervals (67%) correspond to approximately one standard deviation. Nonideality was not considered, as there was no evidence for nonideal effects.

Models incorporating different assembly stoichiometries were based upon the general equation:

$$Y_{(r)} = \delta + \alpha \exp[\sigma(r^2 - r_0^2)] + \sum \alpha^N K_N \exp[N\sigma(r^2 - r_0^2)] \quad (3)$$

where $Y_{(r)}$ is absorbance at radius r, δ the baseline offset, and α the monomer absorbance at reference radius r_0. σ is the reduced molecular weight [$\sigma = M(1 - \bar{v}\varrho)\omega^2/2RT$], N is the stoichiometry of the reaction, and K_N is the association constant of the reaction $NM \leftrightarrow M_N$. σ was fixed at the appropriate value on the basis of the monomer molecular weight and sample conditions. Resolved K_N's were converted to molar association constants on the basis of the calculated ϵ_{280}. Calculations of extinction coefficients at other wavelengths were based upon the absorbance ratio of the same equilibrium data set at 280 nm and the wavelength of interest. Free energies of assembly were calculated by the relationship $\Delta G_N = -RT \ln K_N$.

RESULTS

Stoichiometry of Self-Assembly Reaction. λ cI N-terminal domain self-assembly was studied by sedimentation equilibrium. Figure 2 shows the sedimentation equilibrium data at pH 7, 200 mM KCl, and 20 °C. This consists of three different protein concentrations equilibrated at three different rotor speeds as described in Materials and Methods. Least-squares analysis of each individual data set for its respective weight average molecular weight is presented in Table 2. It is evident that dimer is not an end-product, limiting species since the apparent molecular weight approaches ~27 000. However, it is also evident that N-terminal domains do not go to complete monomer even at the lowest concentration studied. In order to resolve the stoichiometry of self-assembly, the data were analyzed by fitting to several models of self-assembly: either discrete, limited assembly models or an isodesmic model allowing unlimited assembly. The molecular weight was fixed at 11 328 [a] for all fits. The

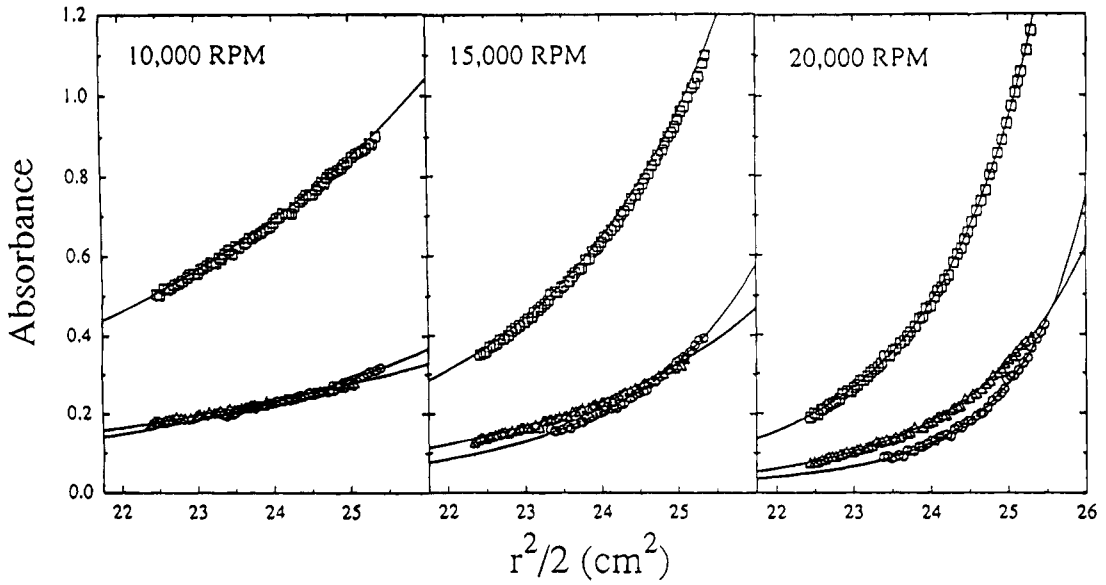

FIGURE 2: Sedimentation equilibrium data for N-terminal domains, plotted as absorbance as a function of $r^2/2$. Conditions were pH 7, 200 mM KCl, and 20 °C. Symbols represent each concentration: (○) 400 μM (scanned at 290 nm); (□) 120 μM (scanned at 280 nm); (△) 40 μM (scanned at 280 nm). Panels represent runs at different speeds: 10 000, 15 000, and 20 000 rpm. Solid lines represent the best fit model (monomer−dimer−tetramer assembly) from simultaneous analysis of all nine data sets. Only every fourth data point is shown.

Table 3: Resolved Free Energies of Self-Assembly for N-Terminal Domains from Fits to Different Self-Assembly Models[a]

stoichiometric model	ΔG_{di}	ΔG_{tri}	ΔG_{tet}	s^b
monomer				4.49e-3
2M−dimer	−5.0 ± 0.1			3.98e-3
3M−trimer		−9.2 ± 0.1		4.11e-3
2M−dimer 3M−trimer	−4.6 ± 0.1	−9.2 ± 0.1		3.82e-3
2M−dimer 4M−tetramer	−4.8 ± 0.1		−13.8 ± 0.1	3.75e-3
M−D−Tri−Tet (isodesmic)	−5.1 ± 0.1			3.88e-3

[a] Data were analyzed according to eq 3. Molecular weight was fixed at monomer M_r = 11 328. Conditions were pH 7, 200 mM KCl, and 20 °C. Free energies were resolved from simultaneous analysis of nine data sets (represented in Figure 2). [b] kcal/mol ± 67% confidence intervals. [c] Square root of variance.

set of ln(K_N) were treated as adjustable parameters according to each particular stoichiometric model. Table 3 contains the results of these fits. As judged by the square root of the variance, all models incorporating a monomer−dimer self-assembly reaction fit the data reasonably well. Models of only monomer formation or monomer−trimer assembly were discarded on the basis of the relatively poor square root of the variance as well as distribution of residuals (data not shown). It was found that those models which included a term beyond dimer (in this case either trimer or tetramer) resulted in a slightly better fit. Although this could be due to adding another parameter to the analysis, inspection of Table 2 indicates an average molecular weight well outside that for dimer. Further, under all conditions studied, the average molecular weight surpassed the dimeric molecular weight value. However, due to lack of extensive data at higher concentrations, it was difficult to resolve the exact stoichiometric reaction. At all conditions studied, the monomer−dimer−tetramer model always fit the data better than monomer−dimer−trimer but only slightly. As can be seen in Table 3, the energetics of self-assembly for trimer or tetramer are very similar in terms of a "per monomer" basis, i.e., the free energy of adding successive monomers. This result led us to evaluate the isodesmic assembly model for domain assembly. As reflected in the square root of the variance, however, the isodesmic model does not offer a superior fit (although the isodesmic model is slightly better at describing the data compared to the simple monomer−dimer model, again indicative of assembly past dimer).

Regardless of the stoichiometric model employed, the energetics of dimerization were essentially constant (see Table 3). Analysis of subsets of data (for example, simultaneous analysis of data collected at one speed) resulted in similar resolved parameters compared to the global fit. These results are also in close agreement with previous estimates of dimerization energetics (Weiss et al., 1987). This gives us confidence that a monomer−dimer reaction was indeed occurring regardless of what the higher order assembly reaction model was. There was a slight dependence on the weight average molecular weight as a function of rotor speed, indicative of a not perfectly reversible thermodynamic system. However, this did not affect the resolved parameters.

pH Effects. The effect of protons on the dimerization of N-terminal domains is shown in Figure 3. There is only a slight pH dependence on the self-assembly of N-terminal domains. The effect is most pronounced in the acidic pH range, indicative of acidic group titration. Over the limited range employed, the data justify fitting to a straight line, with a slope corresponding to a net absorption of 0.4 ± 0.3 proton over the pH range of 5−9.

KCl Dependence. N-Terminal domains show no dependence on KCl concentration over the limited range studied (Figure 4; Table 4): the resolved dimerization free energy is constant at ~4.8 kcal/mol over the range 50−200 mM KCl. From the Wyman derivative relationship, $\Delta\nu_{KCl} = d \ln K/d \alpha_{KCl}$ (Wyman, 1964), the slope of the line describing the salt dependence of N-terminal domain dimerization is directly proportional to the net number of ions released. Over this limited range, the net number of ions released is 0.1 ± 0.4.

Temperature Effects. There is a strong temperature dependence of the dimerization free energy over the range

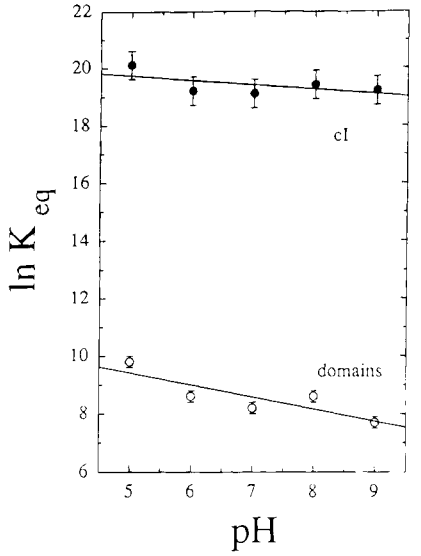

FIGURE 3: Proton-linked effects on N-terminal domain dimerization (○) and cI repressor dimerization (●). Conditions were 200 mM KCl at 20 °C. Solid lines correspond to the net number of protons absorbed, $\Delta\nu_{H^+} = d \ln K/d\alpha_{H^+}$ (Wyman, 1964). Error bars correspond to 67% confidence intervals. See Table 4 for summary of free energies. See Table 7 for net number of protons absorbed. [cI repressor dimerization free energies were determined using analytical gel permeation chromatography (Koblan & Ackers, 1991a).]

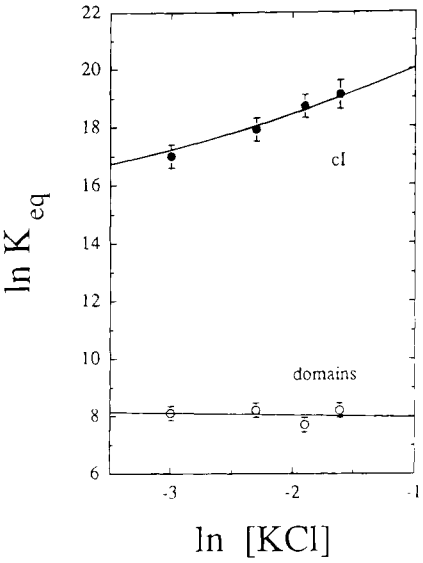

FIGURE 4: KCl-linked effects on N-terminal domain dimerization (○) and cI repressor dimerization (●). Conditions were pH 7, 20 °C. Solid lines correspond to the net number of ions released, $\Delta\nu = d \ln K/d\alpha$ (Wyman, 1964). Error bars correspond to 67% confidence intervals. See Table 4 for summary of free energies. See Table 6 for net number of ions released. [cI repressor dimerization free energies were determined using analytical gel permeation chromatography (Koblan & Ackers, 1991a).]

5−40 °C (Figure 5; Table 4). Within error, dimer formation as a function of temperature is linear over the range studied, thus providing no evidence of a heat capacity effect. The resolved van't Hoff enthalpy is +10.7 ± 2.9 kcal/mol. The entropic contribution ($T\Delta S$) is then +15.8 kcal/mol. This heat is in sharp contrast to the ΔH of intact repressor assembly determined by Koblan and Ackers (1991a) α (−16 kcal/mol).

There was concern that the values determined at 37 and 40 °C might be suspect due to denaturation or degradation

Table 4: Proton, Temperature, and [KCl] Effects on N-Terminal Domain Dimerization[a]

pH	ΔG	s × 10^{-4}	T (°C)	ΔG	s × 10^{-4}	[KCl] (mM)	ΔG	s × 10^4
5	−5.7 ± 0.1	6.9	40	−6.0 ± 0.1	4.0	50	−4.7 ± 0.1	6.3
6	−5.0 ± 0.1	3.9	37	−5.3 ± 0.1	4.2	100	−4.8 ± 0.1	5.8
7	−4.8 ± 0.1	3.8	30	−5.5 ± 0.1	4.3	150	−4.5 ± 0.1	3.9
8	−5.0 ± 0.1	6.4	25	−5.1 ± 0.1	4.2	200	−4.8 ± 0.1	3.8
9	−4.5 ± 0.1	5.9	20	−4.8 ± 0.1	3.8			
			15	−4.7 ± 0.1	4.4			
			10	−4.1 ± 0.1	4.4			
			5	−3.9 ± 0.1	4.9			

[a] Standard Gibbs energies (in kcal/mol ± 67% confidence intervals) for repressor dimerization reaction, obtained by simultaneous analysis of nine channels. Data fit to a 4M−2D−tetramer model. *s* is the square root of the variance.

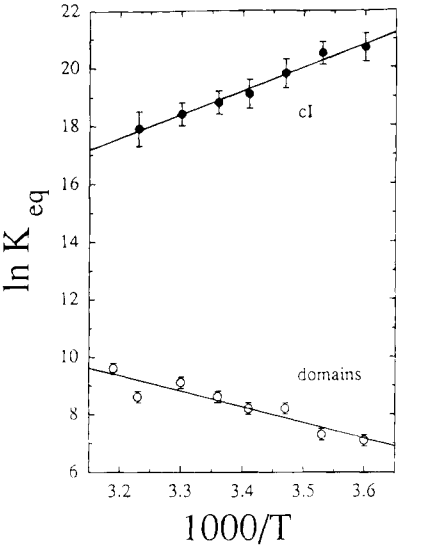

FIGURE 5: Temperature-linked effects of N-terminal domain dimerization (○) and cI repressor dimerization (●). Conditions were 200 mM KCl at pH 7. Solid lines correspond to van't Hoff enthalpies ($d \ln K/dT = \Delta H/RT^2$). Error bars correspond to 67% confidence intervals. See Table 4 for summary of free energies. See Table 6 for van't Hoff enthalpies. [cI repressor dimerization free energies were determined using analytical gel permeation chromatography (Koblan & Ackers, 1991a).]

from being exposed to high temperature for at least 24 h. In order to control for possible denaturation, after the samples were centrifuged and equilibrated at either 37 or 40 °C, the same samples were cooled to 5 °C and allowed to reach sedimentation equilibrium. A dimerization free energy at 5 °C was then determined and compared to an independent determination at 5 °C using fresh protein. The two experiments resolved the same value within error (data not shown).

Footprint Titrations. Results of footprint titration studies as a function of pH, temperature, and salt are given in Table 5. A striking result is that N-terminal domains bind noncooperatively under all conditions studied. The shape of the binding isotherms also supports the noncooperative behavior (see Figure 1). Finally, a minimum in the variance was reached only when the system was allowed to resolve cooperative terms equal to zero.

pH Results. Results of the proton dependence are shown in Figure 6 and Table 5. The free energies of intrinsic binding and cooperative interactions were resolved by simultaneous analysis of duplicate footprint titrations of wild-type operator, and the reduced valency operators O_R1- and

Table 5: Proton, KCl, and Temperature Linkages of Microscopic Gibbs Energies of N-Terminal Domain−O_R Binding[a]

conditions	ΔG_1	ΔG_2	ΔG_3	ΔG_{12}	ΔG_{23}	s^b
pH						
5	−15.3 ± 0.3	−12.7 ± 0.3	−11.9 ± 0.3	−0.1 ± 0.4	−0.2 ± 0.5	0.091
6	−13.6 ± 0.3	−11.2 ± 0.2	−10.0 ± 0.2	+0.3 ± 0.3	+0.1 ± 0.5	0.069
7	−12.6 ± 0.3	−10.7 ± 0.2	−9.4 ± 0.2	+0.2 ± 0.4	+0.1 ± 0.4	0.080
8	−12.5 ± 0.2	−10.0 ± 0.1	−8.9 ± 0.2	+0.1 ± 0.2	+0.4 ± 0.3	0.043
[KCl] (mM)						
200	−12.6 ± 0.3	−10.7 ± 0.2	−9.4 ± 0.2	+0.2 ± 0.4	+0.1 ± 0.4	0.080
150	−13.4 ± 0.3	−11.0 ± 0.3	−9.9 ± 0.4	0	0	0.081
100	−14.2 ± 0.2	−11.8 ± 0.2	−10.9 ± 0.3	0	0	0.073
50	−15.6 ± 0.3	−13.1 ± 0.3	−12.3 ± 0.2	+0.0 ± 0.4	+0.2 ± 0.5	0.092
T (°C)						
37	−12.4 ± 0.1	−10.8 ± 0.1	−9.8 ± 0.1	−0.3 ± 0.2	+0.3 ± 0.3	0.037
30	−12.3 ± 0.2	−10.2 ± 0.1	−9.2 ± 0.2	0	0	0.041
20	−12.6 ± 0.3	−10.7 ± 0.2	−9.4 ± 0.2	+0.2 ± 0.4	+0.1 ± 0.4	0.080
10	−13.2 ± 0.3	−10.4 ± 0.3	−9.5 ± 0.2	0	0	0.096
5	−13.9 ± 0.3	−10.2 ± 0.2	−9.6 ± 0.2	−0.2 ± 0.3	+0.2 ± 0.4	0.079

[a] Standard Gibbs energies (in kcal/mol ±67% confidence intervals) of domain−O_R interactions, obtained by simultaneous analysis of O_R+ and reduced valency mutant binding data (O_R1−, O_R1−,3−) or O_R+ data with ΔG_{ij} terms fixed. [b] Square root of the variance from the simultaneous analysis.

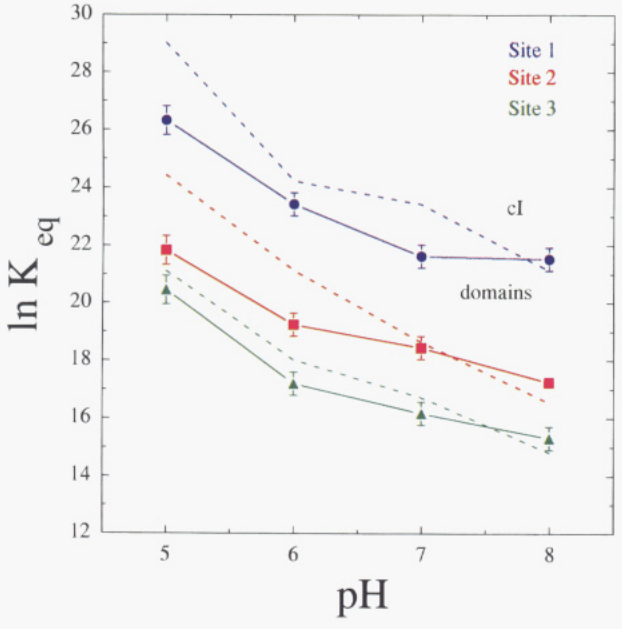

FIGURE 6: Proton-linked effects on free energy of N-terminal domain−O_R binding at 20 °C in 200 mM KCl. Symbols represent microscopic binding constants resolved by simultaneous analysis of O_R+ and reduced valency templates (blue ●, site 1; red ■, site 2; green ▲, site 3). Error bars represent 67% confidence intervals. Slopes of lines correspond to the net number of protons absorbed, $\Delta\nu_{H^+}$ (Wyman, 1964). $d \ln k/d \ln \alpha_{H^+} = (1/2.303RT)[\Delta(\Delta G)/\Delta pH]$. For comparison, analogous results of the proton dependence for intact cI repressor−O_R interactions (Senear & Ackers, 1990) are plotted in dotted lines (blue, site 1; red, site 2; green, site 3). See Table 5 for free energy values. See Table 7 for net number of protons absorbed.

O_R1−,3−, at each pH. At each pH studied, the resolved cooperative terms were zero. Furthermore, a minimum in the variance was found when data were fit to a noncooperative model. At all conditions, high binding specificity was maintained. The order of affinity was constant over the pH range studied (O_R1 > O_R2 > O_R3). All three sites show higher affinity as pH decreases, indicating that protons are absorbed upon ligand binding. The slopes of the curves describing the pH dependencies are directly proportional to the number of protons absorbed. As can be seen in Table 6 within error, the number of protons absorbed is identical for all three sites, although the energetics of binding at site 1 reach a plateau or region of pH independence above pH 7, unlike binding at sites 2 and 3.

Table 6: Proton Absorption Linked to N-Terminal Domain Binding to O_R

	$\Delta\nu_{H^+}$		
pH	O_R1	O_R2	O_R3
5.5	1.3 ± 0.3	1.1 ± 0.3	1.4 ± 0.3
6.5	0.7 ± 0.3	0.4 ± 0.2	0.4 ± 0.2
7.5	0.1 ± 0.3	0.5 ± 0.2	0.4 ± 0.2

Table 7: Thermodynamic Linkages of O_R at pH 7, 20 °C, and 200 mM KCl

system	ΔH (kcal/mol)	$T\Delta S$ (kcal/mol)	$\Delta\nu_{H^+}$ absorbed	$\Delta\nu_{KCl}$ released
O_R1[a]	−27.0	−14.4	0.7	3.7
O_R1[b]	−23.3	−10.1	0.4	3.7
O_R2[a]	−7.4	+3.3	0.4	3.3
O_R2[b]	−14.7	−4.0	1.1	5.2
O_R3[a]	−9.7	+0.3	0.4	3.6
O_R3[b]	−22.7	−12.5	0.6	3.8
cooperativity[a]	0.0	0.0	0.0	0.0
cooperativity[b]	0.0	0.0	0.0	0.0
dimerization[a]	+10.8	+15.6	0.4	0.1
dimerization[b]	−15.9	+4.9	0.3	−1.5

[a] Values for N-terminal domains found in this study. [b] Values for intact cI repressor (Koblan & Ackers, 1992).

KCl Effects. The KCl-dependent affinity of N-terminal domains to O_R is plotted in Figure 7. Affinity at all three sites increases linearly as the KCl concentration decreases. The intrinsic free energies are well resolved, as can be seen by the confidence intervals at each salt concentration. The order of affinity between the three sites is constant over the range of salt concentration (O_R1 > O_R2 > O_R3). At the extremes of salt concentration (50 and 200 mM KCl) there was no evidence for cooperative interactions, thus justifying analysis of only wild-type binding data at intermediate concentrations. Interestingly, there was no evidence of hypersensitivity by cI binding at O_R3 as had been seen by Senear and Batey (1991). The salt dependencies at each site were identical over the range of conditions studied. The slope of the lines is directly proportional to the net number of ions bound or released upon binding. As seen in Table

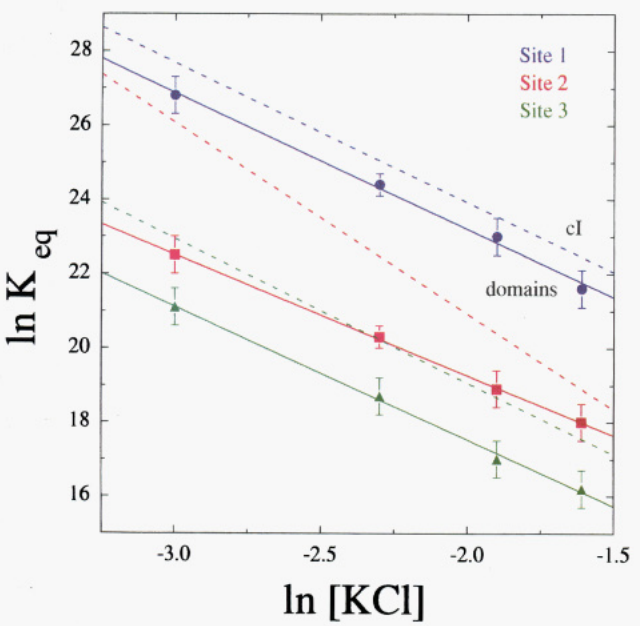

FIGURE 7: KCl-linked effects on free energy of N-terminal domain−O_R binding at pH 7, 20 °C. Symbols represent microscopic binding constants resolved by simultaneous analysis of O_R+ and reduced valency templates (blue ●, site 1; red ■, site 2; green ▲, site 3). Error bars represent 67% confidence intervals. Slopes of lines correspond to the net number of ions released for binding at each site, $\Delta\nu_{KCl}$ ($\Delta\nu_{KCl}$ = d ln K/dα_{KCl}; Wyman, 1964). For comparison, analogous results of the KCl dependence for intact cI repressor−O_R interactions (Koblan & Ackers, 1991b) are plotted in dotted lines (blue, site 1; red, site 2; green, site 3). See Table 5 for summary of free energies. See Table 6 for summary of $\Delta\nu_{KCl}$.

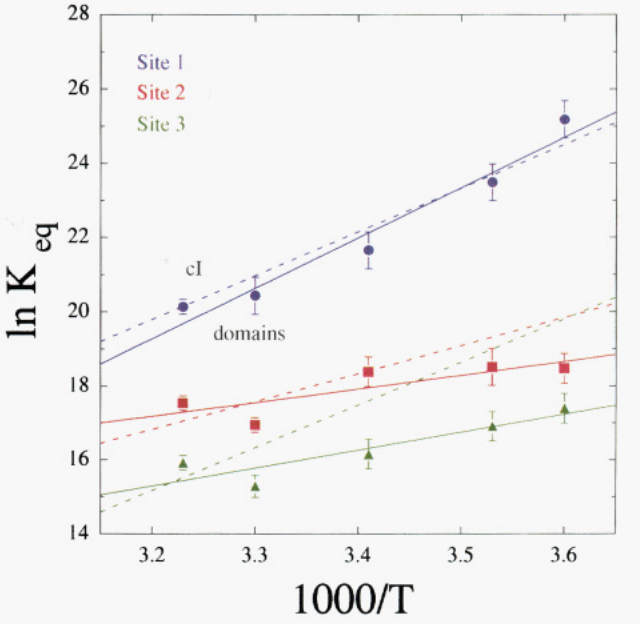

FIGURE 8: Temperature-linked effects on free energy of N-terminal domain−O_R binding at pH 7 in 300 mM KCl. Symbols represent microscopic binding constants resolved by simultaneous analysis of O_R+ and reduced valency templates (blue ●, site 1; red ■, site 2; green ▲, site 3). Error bars represent 67% confidence intervals. Slopes of lines correspond to the van't Hoff enthalpy for binding at each site (d ln K/dT = $\Delta H/RT^2$). For comparison, analogous results of the temperature dependence for intact cI repressor−O_R interactions (Koblan & Ackers, 1992) are plotted in dotted lines (blue, site 1; red, site 2; green, site 3). See Table 5 for summary of free energies. See Table 7 for summary of enthalpies.

7, all three sites release the same number of ions. Nonlinearity would be expected if there were linkages or preferential interactions with Mg^{2+} or Ca^{2+} or if ion release was associated with protein rather than DNA.

Temperature Studies. The results of the temperature dependence of domain binding to O_R are shown in Table 5 and Figure 8. The resolved free energies at 5, 20, and 37 °C were based upon simultaneous analysis of the wild-type operator and reduced valency operators as described in Materials and Methods. The binding free energies determined at 10 and 30 °C were based upon analysis of only wild-type operator binding data; cooperative terms were fixed at zero. There was no evidence of nonspecific binding at any temperature, nor was there any evidence of cooperative interactions at any temperature. As with the pH and salt studies, a minimum in variance was obtained when cooperative terms were set equal to zero. Furthermore, the shape of the isotherms were indicative of noncooperative interactions. Binding affinity increases as the temperature decreases. Intrinsic terms were well resolved, as indicated by the error bars. Again, the order of affinity is constant over the temperature range studied (O_R1 > O_R2 > O_R2). Within error of the data, there appears to be a linear temperature dependence of binding for all three sites, indicating that there is no heat capacity change associated with binding, unlike many other protein−DNA interactions. The slope of the temperature dependence is directly proportional to the apparent heat of binding at each site. As shown in Table 7, the van't Hoff heat of binding for site 1 is large and negative (−27.0 ± 4.9 kcal/mol) though heats at sites 2 and 3 are small and negative (−7.4 ± 4.5 and −9.7 ± 4.1 kcal/mol). By the relationship $\Delta G = \Delta H - T\Delta S$, one can calculate the apparent entropic contribution at standard conditions. As with the enthalpic terms, there is a significant entropic contribution for binding at site 1; however, there is essentially none for binding at sites 2 and 3 (see Table 6).

DISCUSSION

In this study we have employed sedimentation equilibrium and quantitative DNase I footprint titration to study self-assembly and site-specific binding of λ cI N-terminal domains to λ right operator, O_R. Studies of assembly and binding energetics as a function of pH, salt, and temperature may allow determination of the underlying molecular forces responsible for site specificity and cooperativity. At one level, the results presented here confirm and support the general features of N-terminal domain−O_R interactions as described by Ptashne (1986). (Namely, domains undergo an energetically weak monomer−dimer transition, they have similar binding affinities for O_R as for intact cI, and they exhibit no cooperative interactions of the type attributed to intact repressor.) However, these studies of the pH, salt, and temperature dependence of N-terminal domain self-assembly and binding indicate that there are different linkages between these thermodynamic driving forces from those of intact cI. Furthermore, these differences are sequence specific. In other words, cI domains do not act independently, and the nature of their interaction is, at least in part, a function of the DNA sequence. This also implies that the C-terminus plays a role in site discrimination. These results will form the basis of the following discussion, focusing on determining the physicochemical mechanisms underlying biological regulation in protein−DNA assemblies.

Self-Assembly of N-Terminal Domains. Our results suggest that N-terminal self-assembly is predominantly, but not

exclusively, monomer to dimer in the concentration range studied. Dimers are not a limiting species but rather an intermediate along a pathway to trimer or tetramer. The differences in goodness of fit between monomer−dimer−trimer and monomer−dimer−tetramer models were too small to resolve exact stoichiometries beyond the dimeric stage. However, as all evidence suggested dimers to be the active species for DNA binding, the crucial information needed was an accurate free energy of dimer formation. Table 3 indicates that this parameter was, in fact, very insensitive to the different models of stoichiometry. This increases confidence in the accuracy of our dimerization value and supports the idea of self-assembly being dominated by a monomer−dimer process. These results are in agreement with a previous estimate on N-terminal domain assembly (Weiss et al., 1987).

The pH dependence of domain assembly was found identical to that for intact repressor (see Figure 3). This indicates that proton uptake upon DNA binding of the native repressor is associated with the amino terminus and that these events are unaffected by the C-terminal domain. Our results show a shift in pK_a's to more basic values. Although such proton absorption probably reflects several ionizable groups, the observed pattern of pH dependence suggests groups titrating in the pH range 5 to 6 as well as pH 8−9. Possibilities include the terminal amino group (pK_a = 8.0) and the acidic groups aspartate (pK_a = 4.5) and glutamate (pK_a = 4.6). On the basis of the N-terminal domain crystal structure and cocrystal structure (Pabo & Lewis, 1982; Jordan & Pabo, 1988), glutamates 83, 86, and 89 would be likely candidates due to their spatial proximity to the dimerization interface. One obvious candidate would have been the sole histidine residue (pK_a = 6.5) in each monomer of intact cI; however, that histidine is not present in the 1−102 amino acid fragment. Since proton dependencies for intact cI and N-terminal domain assembly are identical, it is unlikely that the histidine plays a role in dimerization. (The histidine could, however, be involved in DNA binding given the differential pH effects between the two proteins; see Results.)

In contrast, the salt dependence is very different between N-terminal domains and intact repressor (see Figure 4). No salt-dependent dimerization of N-terminal domains was observed over the range studied. However, the range is quite limited. Previous studies on intact cI dimerization have implicated an ion binding event (Koblan & Ackers, 1991a). If such an event is involved, it can be assigned to the C-terminal domain only if one assumes that the N-terminal domain was not significantly perturbed.

The temperature dependence of the dimerization reaction is dramatically different from that of intact cI (as seen in Figure 5). Previous studies (Koblan & Ackers, 1991a) demonstrated that intact cI dimerization has an enthalpy of −16 kcal/mol. This contrasts sharply to the behavior of N-terminal domains, for which we find a van't Hoff enthalpy of +11 kcal/mol. These values are also supported by isothermal titration calorimetry studies (data not shown). Two possibilities are of interest: (a) compensation of the large positive enthalpy by a very large negative enthalpy (−27 kcal/mol) at the C-terminal domain, resulting in the net value of −16 kcal/mol; (b) rearrangement of the N-terminal interface upon forming domains from intact repressor. It is difficult to eliminate either of these possibilities. However, given that, once the weak dimerization free energy is accounted for, N-terminal domain binding energetics are very similar to those of intact cI, it seems more likely that possibility a is the correct explanation. It should be noted that this explanation is not compatible with the idea of functionally independent domains.

The N-terminal domain dimerization interface is thought to be defined by the interactions between helix 5 of each monomer (Pabo & Lewis, 1982). These amphipathic helices form a largely hydrophobic interaction. Results of the current study support that hypothesis, in part. The strong positive temperature dependence (resulting in a large and positive enthalpy of association) is consistent with a reaction dominated by hydrophobic interactions. However, another indicator of hydrophobic interactions is a negative heat capacity. Although it is difficult to determine whether there is any curvature to the temperature dependence data (Figure 5), isothermal titration calorimetry studies have yielded a heat of dimer dissociation which agrees with the van't Hoff enthalpy but also indicated a small heat capacity [~0.05 kcal/(mol·T)]. The weak pH and KCl dependencies of the dimerization reaction indicate that electrostatic and ionic effects do not play a dominant role. However, these studies were necessarily conducted over a limited range. Although hydrophobic interactions may dominate the dimerization reaction, other effects probably also contribute. Regardless of the exact set of molecular forces involved, the temperature studies suggest that the dimerization reaction is not controlled exclusively by the C-terminal domain; it is clear that the reaction has a global character.

Cooperative Binding and Linkage. It is found in this work that N-terminal domains are noncooperative under all conditions studied. This supports the long-held notion that cooperative interactions *per se* are localized to the C-terminal domain. At fixed conditions of T, pH, and salt the free energies of binding N-terminal domains to the DNA operator sites distribute in a pattern similar to that of intact repressor, once the weak dimerization free energy is accounted for. This would imply that domains are not significantly altered in their function by loss of the C-terminus. However, the domains do have site-specifically different linkages to protons, ions, and temperature compared with intact repressors, suggesting sequence-specific communication between the two kinds of domains within the cI dimer. A comparative summary of these linkages is given in Table 7.

pH Dependence of Binding. The N-terminal domains maintained the same order of binding affinity for all conditions studied, $O_R1 > O_R2 > O_R3$, and showed no evidence for cooperative interactions. The net proton release ($\Delta\nu_{H^+}$) was calculated by $(1/2.303RT)[\Delta(\Delta G)/\Delta pH]$. The results are shown in Table 7. With the possible exception of low pH, these results must reflect titration of groups associated with N-terminal domains. Within error, binding at each site is accompanied by the same number of protons absorbed; thus one cannot exclude the possibility that the pH dependence is linked solely to titration of free repressor, rather than sequence-dependent shifts in pK_a's as seen in intact repressor binding (Senear & Ackers, 1990). This may imply that the C-terminal domain confers site discrimination upon the intact molecule.

In the pH 7−8 range, a region of pH dependence is reached at site 1; thus the energy difference in going from pH 5 to pH 8 is attributable to proton-linked events. Likewise, a lower limit on proton-linked energetics at sites 2 and 3 can be calculated. These values are, within error,

the same for all three sites: 2.8, 2.7, and 3.0 kcal/mol for sites 1, 2, and 3, respectively.

Comparison of intact repressor pH dependence with that of N-terminal domains indicates a similar binding affinity for all three sites that increases as pH decreases (see Figure 6). The numbers of protons released are very close to those for intact cI, suggesting that they arise from the same ionizable groups and that therefore those groups can be localized to the N-terminal domain (at least for the acidic to neutral region). Secondly, the pH results imply (as do salt and temperature studies) that the N-terminal domains still function upon loss of the C-terminal domain. Thus, cooperativity has been decoupled from site-specific (and probably nonspecific) binding without destroying the protein. This is strong evidence for localizing cooperativity to the C-terminal domain.

An assignment of specific titrating groups is difficult, however; the loss of histidine 108 means that it cannot be contributing to pH effects of N-terminal domain binding (although it may contribute to intact cI binding). This leaves the terminal amino group, glutamates, and aspartates as candidates.

Salt Dependence of Binding. As seen in Figure 7, there is a strong salt dependence on the site-specific binding of domains to O_R. The salt dependence is, within error, linear and identical at all three sites. If the entire salt effect is attributed to KCl-linked interactions, the slopes of these lines translate to 3.7 ion equivalents released upon binding at each site (see Table 7). It should be noted, however, that in principle these slopes should exhibit curvature due to either anion release linked to domain binding (deHaseth et al., 1977; Record et al., 1977, 1978), as well as preferential interactions, or binding of Mg^{2+} and Ca^{2+} [see Lohman (1985)]. However, over this limited range of moderate salt concentration, it is difficult to resolve with certainty any curvature in the data. Identical KCl linkages at each site would imply similar mechanisms of binding. The simplest interpretation of these results is that ions are released from the DNA operator sites. This work be consistent with the identical site sizes of each operator (17 bp), as well as the previously discussed results indicating no ionic linkage to domain dimerization.

In contrast, however, site-specific binding of intact repressor does not result in an identical number of ions released at each site (Koblan & Ackers, 1991; see Figure 6); while ion release associated with binding at sites 1 and 3 was 3.7 ions, release at site 2 was 5.2 ions. That the salt dependence at site 2 changes upon loss of the C-terminal domain (but not at sites 1 and 3) would implicate that domain in ion-linked effects, but more importantly, it implies that the C-terminus plays a role in site-specific discrimination.

Temperature Studies. Footprint titration studies as a function of temperature indicate that all three sites have temperature-dependent binding energetics. Unlike the KCl-linked effects, however, the enthalpic contributions derived from the temperature studies reveal a dramatic difference between temperature effects at site 1 compared to temperature effects at sites 2 and 3 (see Figure 8). van't Hoff analysis of the resolved binding free energies indicates enthalpies of binding of −27 kcal/mol at site 1, −7.4 kcal/mol at site 2, and −9.7 kcal/mol at site 3. (As in the KCl studies, there was no evidence of cooperative interactions; thus there was no measured heat of cooperativity.) Of interest is the change in enthalpies at each site when compared to results from temperature dependence of intact cI−O_R interactions (Koblan & Ackers, 1992). Analogous to studies on KCl dependence of binding (Koblan & Ackers, 1991b), a striking result was an identical large and negative enthalpy for binding sites 1 and 3 and a smaller (but still negative) enthalpy for site 2. In the current study, that trend has disappeared. Both intact cI and N-terminal domains have the same enthalpy of binding at site 1, yet distinctly different enthalpies when they bind to sites 2 and 3. Furthermore, the small enthalpies of binding at sites 2 and 3 translate to small entropies of binding. By consequence there is no net entropic contribution to binding even though we expect the observed release of 3.7 ions to be an inherently entropic event.

The negative enthalpies of binding are consistent with protonation events as seen in the pH studies. However, if the entire enthalpic contribution for saturating the three sites of O_R (−45 kcal/mol) is attributed to the total proton absorption at O_R (1.5 protons), then the heat of protonation would be −30 kcal/mol, well beyond any measured value for an individual amino acid protonation event. Furthermore, on a site by site basis, there is a highly nonlinear response: −27 kcal/mol for 0.7 proton, −9 kcal/mol for 0.4 proton, and −8 kcal/mol for 0.4 proton. Thus, other forces must certainly be coupled to proton absorption (and ion release), possibly including van der Waals forces, hydrophobic interactions, and conformational changes. As with the salt studies, there appears to be a weak correlation between changes in protein (intact cI to solely N-terminal domain) and changes in linkages between sites. This set of results may then point toward sequence-specific, conformationally dependent interactions that make it difficult to envision simple rules. This set of results also makes it difficult to think about protein−DNA interactions in terms of a sum of local interactions but rather that they must include a global component. Raman spectroscopic studies (Benevides et al., 1991), the cI−O_L1 cocrystal structure (Jordan & Pabo, 1988), and the cro cocrystal structure (Brennan et al., 1990) all indicate that both protein and DNA exhibit plasticity upon complex formation. This work supports those mechanistic features and also suggests that they are sequence specific.

REFERENCES

Babul, J., & Stellwagon, E. (1969) *Anal. Biochem. 28*, 216−221.

Backman, K., Ptashne, M., & Gilbert, W. (1976) *Proc. Natl. Acad. Sci. U.S.A. 73*, 4174−4178.

Beckett, D., Burz, D. S., Ackers, G. K., & Sauer, R. T. (1993) *Biochemistry 32*, 9073−9079.

Benevides, J. M., Weiss, M. A., & Thomas, G. J., Jr. (1991) *Biochemistry 30*, 5955−5963.

Box, G. D. P. (1960) *Ann. N.Y. Acad. Sci. 86*, 792.

Brennan, R. C., Roderick, S. L., Takeda, Y., & Mathews, B. (1990) *Proc. Natl. Acad. Sci. U.S.A. 87*, 8165−8169.

Brenowitz, M., Senear, D. F., Shea, M. A., & Ackers, G. K. (1986) *Methods Enzymol. 130*, 132−181.

Burz, D. S., & Ackers, G. K. (1994) *Biochemistry 33*, 8406−8416.

Burz, D. S., Beckett, D., Benson, N., & Ackers, G. K. (1994) *Biochemistry 33*, 8399−8405.

Cohn, E. J., & Edsall, J. T. (1943) *Proteins, Amino Acids and Peptides as Ions and Dipolar Ions*, Reinhold, New York.

deHaseth, P. L., Lohman, T. M., & Record, M. T., Jr. (1977) *Biochemistry 16*, 4783−4790.

Johnson, A. D., Meyer, B. J., & Ptashne, M. (1979) *Proc. Natl. Acad. Sci. U.S.A. 76*, 5061−5065.
Johnson, M. L., & Frasier, S. G. (1985) *Methods Enzymol. 117*, 301−342.
Johnson, M. L., Correia, J. C., Yphantis, D. A., & Halvorson, H. R. (1981) *Biophys. J. 36*, 575−588.
Jordan, S. R., & Pabo, C. O. (1988) *Science 242*, 893−899.
Koblan, K. S., & Ackers, G. K. (1991a) *Biochemistry 30*, 7817−7821.
Koblan, K. S., & Ackers, G. K. (1991b) *Biochemistry 30*, 7822−7827.
Koblan, K. S., & Ackers, G. K. (1992) *Biochemistry 31*, 57−65.
Lohman, T. M. (1985) *CRC Crit. Rev. Biochem. 19*, 191−245.
Maniatis, T., Fritsch, E. F., & Sambrook, J. (1982) *Molecular Cloning: A Laboratory Manual*, Cold Spring Harbor Laboratory, Cold Spring Harbor, NY.
Meyer, B. J., Maurer, R., & Ptashne, M. (1980) *J. Mol. Biol. 139*, 163−194.
Pabo, C. O., & Lewis, M. (1982) *Nature 298*, 443−447.
Ptashne, M. (1986) *The Genetic Switch*, Cell Press, Cambridge, MA.
Record, M. T., Jr., deHaseth, P. L., & Lohman, T. M. (1977) *Biochemistry 16*, 4791−4796.
Record, M. T., Jr., Anderson, C. F., & Lohman, T. M. (1978) *Q. Rev. Biophys. 11*, 103−178.
Sauer, R. T., Hehir, K., Stearman, R. S., Weiss, M. A., Jeitler-Nilsson, A., Suchanek, E. G., & Pabo, C. O. (1986) *Biochemistry 25*, 5992−5998.
Senear, D. F., & Ackers, G. K. (1990) *Biochemistry 29*, 6568−6577.
Senear, D. F., & Batey, R. (1991) *Biochemistry 30*, 6677−6688.
Shea, M. A. (1983) Ph.D. Dissertation, Johns Hopkins University, Baltimore, MD.
Weiss, M. A., Pabo, C. O., Karplus, M., & Sauer, R. T. (1987) *Biochemistry 26*, 897−904.
Wiseman, T., Williston, S., Brandts, J. F., & Lin, L. N. (1989) *Anal. Biochem. 179*, 131−137.
Wyman, J., Jr. (1964) *Adv. Protein Chem. 19*, 224−394.